New Phytologist

Research

Dissecting the impact of CO_2 and pH on the mechanisms of photosynthesis and calcification in the coccolithophore *Emiliania huxleyi*

Lennart T. Bach[1,*], Luke C. M. Mackinder[1,2,4,*], Kai G. Schulz[1], Glen Wheeler[2,3], Declan C. Schroeder[2], Colin Brownlee[2] and Ulf Riebesell[1]

[1]Helmholtz-Zentrum für Ozeanforschung Kiel (GEOMAR), D-24105, Kiel, Germany; [2]Marine Biological Association of the UK, The Laboratory, Citadel Hill, Plymouth, PL1 2PB, UK; [3]Plymouth Marine Laboratory, Prospect Place, Plymouth, PL1 3DH, UK; [4] Present address: Department of Plant Biology, Carnegie Institution, 260 Panama Street, Stanford, CA 94305, USA

Author for correspondence:
Luke C. M. Mackinder
Tel: +1 650 739 4292
Email: lukemack@stanford.edu

Received: *10 December 2012*
Accepted: *8 February 2013*

New Phytologist (2013)
doi: 10.1111/nph.12225

Key words: calcification, carbon-concentrating mechanisms (CCMs), climate change, coccolithophores, *Emiliania huxleyi*, ocean acidification, phytoplankton.

Summary

- Coccolithophores are important calcifying phytoplankton predicted to be impacted by changes in ocean carbonate chemistry caused by the absorption of anthropogenic CO_2. However, it is difficult to disentangle the effects of the simultaneously changing carbonate system parameters (CO_2, bicarbonate, carbonate and protons) on the physiological responses to elevated CO_2.
- Here, we adopted a multifactorial approach at constant pH or CO_2 whilst varying dissolved inorganic carbon (DIC) to determine physiological and transcriptional responses to individual carbonate system parameters.
- We show that *Emiliania huxleyi* is sensitive to low CO_2 (growth and photosynthesis) and low bicarbonate (calcification) as well as low pH beyond a limited tolerance range, but is much less sensitive to elevated CO_2 and bicarbonate. Multiple up-regulated genes at low DIC bear the hallmarks of a carbon-concentrating mechanism (CCM) that is responsive to CO_2 and bicarbonate but not to pH.
- *Emiliania huxleyi* appears to have evolved mechanisms to respond to limiting rather than elevated CO_2. Calcification does not function as a CCM, but is inhibited at low DIC to allow the redistribution of DIC from calcification to photosynthesis. The presented data provides a significant step in understanding how *E. huxleyi* will respond to changing carbonate chemistry at a cellular level.

Introduction

Marine photoautotrophic organisms fix *c.* 55 gigatonnes of carbon yr^{-1} which is equal to the photosynthetic production by the terrestrial biosphere (Field *et al.*, 1998). Coccolithophores play a major role in the global carbon cycle by contributing *c.* 1–10% to total organic carbon fixation (Poulton *et al.*, 2007) and providing ballast through the formation of calcite, which enhances organic matter sinking into the deep ocean (Thierstein *et al.*, 1977). The globally most abundant coccolithophore species is *Emiliania huxleyi*, which has the ability to form blooms up to 8×10^6 km^2 (Moore *et al.*, 2012). Despite the global significance of *E. huxleyi*, there is only a limited understanding of important cellular processes and their response to environmental change.

Under present-day conditions, marine phytoplankton growth is mostly limited by low light availability or by the insufficient supply of inorganic nutrients, such as nitrogen, phosphorus or iron (Sarmiento & Gruber, 2006), while carbon dioxide (CO_2) is usually not considered to be limiting. Nevertheless, CO_2 diffusion rates are in most cases not high enough to account for the photosynthetic rates seen in the majority of phytoplankton (Falkowski & Raven, 2007). This discrepancy is explained by the action of carbon (or CO_2) concentrating mechanisms (CCMs). In algae these are predominantly C3 biophysical mechanisms which link carbonic anhydrases (CAs), dissolved inorganic carbon (DIC) transporters and pH gradients to enhance [CO_2] at the active site of Ribulose-1,5-bisphosphate carboxylase oxygenase (RubisCO) (Reinfelder, 2011). It is thought that nearly all marine phytoplankton operate a CCM, although the DIC species used (CO_2 and/or bicarbonate (HCO_3^-)), its regulation, cellular components, and DIC affinity can vary significantly between species (Giordano *et al.*, 2005). *E. huxleyi* operates a low-affinity CCM (Rost *et al.*, 2003). Several studies indicate that CO_2 is the primary source for photosynthesis, although there are some discrepancies over the importance of HCO_3^-, especially at lower CO_2 concentrations (Paasche, 1964; Sikes *et al.*, 1980; Nimer & Merrett, 1992; Sekino & Shiraiwa, 1994; Herfort *et al.*, 2002; Rost *et al.*, 2003; Schulz *et al.*, 2007; Bach *et al.*, 2011). In

*These authors contributed equally to this work.

addition to a biophysical mechanism, intracellular calcification has been proposed to act as a CCM by providing protons (H^+) as a by-product of calcification to support the dehydration of HCO_3^- to CO_2 (reviewed in; Paasche, 2001). Although there are some supporting data (Nimer & Merrett, 1992; Buitenhuis *et al.*, 1999), other studies contradict the concept (Paasche, 1964; Herfort *et al.*, 2004; Trimborn *et al.*, 2007; Leonardos *et al.*, 2009).

In the forthcoming centuries, ongoing uptake of anthropogenic atmospheric CO_2 into the oceans will continuously change the marine carbonate chemistry – a process known as ocean acidification (Caldeira & Wickett, 2003). Chemically, ocean acidification leads to a strong decrease of the carbonate ion (CO_3^{2-}) concentration, a slight increase in [HCO_3^-] and a strong increase in [CO_2] and [H^+] (Wolf-Gladrow *et al.*, 1999). These components are thought to affect coccolithophores in varying ways, with [CO_3^{2-}] influencing calcite saturation concentrations, [H^+] affecting cellular pH homeostasis, [CO_2] affecting photosynthesis and [HCO_3^-] influencing calcification (and photosynthesis). The potential effects of ocean acidification on calcification and photosynthesis by *E. huxleyi* have been repeatedly reported (reviewed in Riebesell & Tortell, 2011), but the importance of changes in the individual carbonate parameters for the observed responses is still not fully understood.

The present study disentangles the carbonate system to improve our conceptual understanding of the acquisition of DIC and its subsequent use in calcification and photosynthesis. In particular, we address two important questions in *E. huxleyi* ecophysiology: how sensitive is *E. huxleyi* to low and elevated components of the carbonate system; and does calcification act as a CCM?

Materials and Methods

Conceptual background of the experiments

The marine carbonate system is defined by the concentrations of CO_2, HCO_3^-, CO_3^{2-}, pCO_2, total alkalinity (TA), DIC (i.e. combined CO_2, HCO_3^- and CO_3^{2-}), and pH ([H^+]; Zeebe & Wolf-Gladrow, 2001). The physiologically relevant parameters of the carbonate system are CO_2, HCO_3^-, CO_3^{2-} and H^+, as only these can be perceived by a cell. They are connected to each other in the equilibrium reaction:

$$CO_2 + H_2O \Leftrightarrow HCO_3^- + H^+ \Leftrightarrow CO_3^{2-} + 2H^+ \qquad \text{Eqn 1}$$

As no other parameters of physiological relevance other than CO_2, HCO_3^-, CO_3^{2-} and H^+ were changed in the experiments (e.g. light or temperature), it is assumed that only changing concentrations of these particular parameters can induce physiological or genetic responses. CO_2, HCO_3^-, CO_3^{2-} and H^+ are closely codependent (Eqn 1) and any change in the concentration of one will lead to changes in the others. Nevertheless, it is possible to keep one of the four parameters constant while changing the other three. We made use of this feature and performed three experiments where we kept either [CO_2] or [H^+] constant between treatments ([H^+] was kept constant at two different concentrations). The constant carbonate system parameter within an experiment can be excluded from being responsible for the observed physiological or genetic response (Buitenhuis *et al.*, 1999). Note that we chose to focus on CO_2 and H^+, as previous work points towards a primary importance of these particular parameters for *E. huxleyi* physiology (Schulz *et al.*, 2007; Bach *et al.*, 2011).

Experimental design and basic setup

Three experiments were conducted to test the physiological and molecular responses of *Emiliania huxleyi* (Lohmann) Hay and Mohler to changes in individual carbonate chemistry parameters. DIC was varied in all experiments, while either pH_f (8.34 or 7.74 on free scale) or CO_2 (16 μmol kg^{-1}) was kept constant. In all experiments, cells of *E. huxleyi* (strain B92/11) were grown in monoclonal dilute batch cultures (LaRoche *et al.*, 2010) at 15°C and 150 μmol m^{-2} s^{-1} incident photon flux density under a 16 : 8 h, light: dark cycle. The growth medium was artificial seawater prepared as described in Kester *et al.* (1967) but without the addition of $NaHCO_3$, which was added in a later step (see the following section). Artificial seawater was enriched with *c.* 64 μmol kg^{-1} nitrate, 4 μmol kg^{-1} phosphate, f/8 concentrations of a trace metal and vitamin mixture (Guillard & Ryther, 1962), 10 nmol kg^{-1} of SeO_2, and 2 ml kg^{-1} of natural North Sea water. Concentrations of nitrate and phosphate were measured according to Hansen & Koroleff (1999). The nutrient-enriched artificial seawater was sterile-filtered into polycarbonate bottles where the carbonate chemistry was manipulated. After taking samples for carbonate chemistry measurements (see the following section), the artificial seawater was divided carefully into three 2.3 l polycarbonate bottles before inoculation. Before inoculation, *E. huxleyi* cells were acclimated to exponential growth and carbonate chemistry conditions for at least seven generations. Approximate cell densities ranged from 50 to 300 cells ml^{-1} at inoculation and 40 000–100 000 cells ml^{-1} at sampling (see description of sampling later).

Carbonate chemistry manipulation and determination

In all experiments, target DIC concentrations were adjusted by adding calculated amounts of $NaHCO_3$ or Na_2CO_3 (see Bach *et al.*, 2012 for details). In the constant-CO_2 experiment, CO_2 was set to a constant concentration of *c.* 16 (± 2) μmol kg^{-1} through additions of calculated amounts of HCl (3.571 molar). In the constant-pH experiments, pH was adjusted to 7.74 (± 0.004) or 8.34 (± 0.008) by adding 2 mmol kg^{-1} of 2-[-4-(2-hydroxyethyl)-1-piperazinyl]-ethanesulfonic acid (HEPES, adjusted to target pH_f levels).

Carbonate chemistry in the constant-CO_2 experiment was determined by measuring TA and pH_f, while in both constant-pH experiments it was determined from pH_f and DIC. Carbonate chemistry samples were taken at the beginning and the end of the experiments. Samples for TA were filtered (0.7 μm), poisoned with saturated $HgCl_2$ solution (0.5‰ final concentration) and stored at 4°C until measured (Dickson *et al.*, 2003). TA values higher than

4700 μmol kg^{-1} were outside the range that can be accurately determined with the applied method and therefore diluted with double deionized water as described in Bach *et al.* (2012).

Samples for DIC were sterile-filtered (0.2 μm) by gentle pressure into 4 ml borosilicate bottles, made air-tight without headspace and subsequently measured as described in Stoll *et al.* (2001). DIC samples lower than 1000 or higher than 3000 μmol kg^{-1} could not be reliably measured with the applied method and were therefore either diluted or concentrated (see Bach *et al.*, 2011, 2012).

Samples for pH_f were measured potentiometrically at 15°C with separate glass and reference electrodes (METROHM) calibrated with reference seawater, certified for TA and DIC (supplied by Prof. A. Dickson, La Jolla, CA, USA; see Bach *et al.*, 2011, 2012 for details).

Carbonate chemistry parameters that were not directly measured were calculated from two measured values (DIC and TA or DIC and pH_f) and known salinity, temperature, and phosphate concentrations with the software CO2SYS (Lewis & Wallace, 1998) using equilibrium constants determined by Roy *et al.* (1993). Biological response data are plotted against the means of the initial and final values of the carbonate chemistry. Error bars in plotted carbonate chemistry parameters denote the mean change of the three replicates of the particular carbonate chemistry parameter from the beginning of the experiment to the end.

Sampling, measurements and calculations of growth, organic, and inorganic carbon production rates

Sampling started 2 h after the onset of the light period and lasted not longer than 2.5 h. Duplicate samples for total particulate carbon (TPC) and particulate organic carbon (POC) were filtered (200 mbar) on to precombusted (5 h at 500°C) GF/F filters. To remove HEPES from the filters of the constant-pH experiments, samples were rinsed with 60 ml of artificial seawater medium supersaturated with respect to calcium carbonate and free of HEPES buffer immediately after filtration. Filters were stored at −20°C until measurements were carried out. POC filters were placed for 2 h in a desiccator containing fuming HCl to remove all calcite and then dried for *c.* 6 h at 60°C. TPC filters were dried under the same conditions but without the acid treatment. TPC and POC analyses were performed using an elemental analyzer (HEKATECH, Wegberg, Germany) combined with an isotope ratio mass spectrometer (FINNIGAN, Schwerte, Germany). Particulate inorganic carbon (PIC) was calculated as the difference between TPC and POC.

Cell numbers were determined with a Coulter Counter (Beckman Coulter, Krefeld, Germany) at the beginning and the end of the experiments *c.* 4 h after the onset of the light period. Growth rates (μ) were calculated as

$$\mu = \frac{\log_e(t_{fin}) - \log_e(t_0)}{d} \qquad \text{Eqn 2}$$

where t_0 and t_{fin} are the cell numbers at the beginning and the end of the experiments, respectively, and d is the growth period in days. POC and PIC production rates were calculated by multiplying growth rates with the cellular POC or PIC contents.

Treatments were further analyzed by scanning electron microscopy (SEM) and cross-polarized light microscopy to confirm the presence or absence of internal coccoliths (Bach *et al.*, 2012). Cells were considered to be actively calcifying if coccoliths were present.

For gene expression analysis, *c.* 10 million cells were filtered (200 mbar) onto polycarbonate filters with a pore size of 0.8 μm and subsequently rinsed off the filters with 1 ml RNAlater (Qiagen). This cell suspension was kept on ice until storage at −20°C.

Quantitative reverse-transcriptase polymerase chain reaction (qRT-PCR)

Quantitative reverse-transcriptase polymerase chain reaction was performed for 15 target genes (Table 1). Each sample was measured in triplicate. Experimental procedures were performed as described previously (Mackinder *et al.*, 2011). Primers were designed using expressed sequence tag (EST) clusters from von Dassow *et al.* (2009), the *E. huxleyi* Genome Project (http://genome.jgi-psf.org/Emihu1/Emihu1.home.html) or from the current literature (Supporting Information, Table S1). Efficiency curves for each primer pair were generated using serial dilutions on pooled cDNA from all samples. All primers except beta-carbonic anhydrase (βCA) had efficiencies between 90 and 105% and generated curves with R^2 values > 0.99. βCA efficiency remained undetermined as a result of the low cycle threshold (C_T) values of pooled cDNA even at undiluted levels. For relative expression calculations, its efficiency was assumed to be 100%. This assumption results in a potential decrease in the accuracy of the absolute fold changes, but the trend of expression and the order of magnitude will remain unaffected. For each sample, 2–20 ng of RT RNA were analyzed in technical triplicates. For each primer pair, all samples were analyzed across three plates, and in order to allow for the correction of between-plate variation two standards in triplicate were run on each plate. GeNorm (Vandesompele *et al.*, 2002) was used to test the stability of four potential endogenous reference genes (ERGs).

Analysis of qRT-PCR data was done using an efficiency-corrected $\Delta\Delta C_t$ method, normalizing to the geometric mean of three ERGs (Vandesompele *et al.*, 2002). For each gene, all samples were plotted relative to the sample with lowest expression from all three experiments. The sample with the lowest expression level was normalized to 1, allowing the expression ratios between samples to be easily identified.

Statistical analysis

We tested if the carbonate chemistry had a statistically significant effect ($P < 0.05$) on individual physiological and molecular response parameters with either a one-factorial analysis of variance (ANOVA) using Statistica (Statsoft, Hamburg, Germany) in case the data subsets were normally distributed, or with a permutational multivariate analysis of variance (PERMANOVA) using Primer 6 in case they were not. Normality was tested with

New Phytologist (2013)
www.newphytologist.com

Table 1 *Emiliania huxleyi* genetic response to carbonate system manipulations

		Correlation to carbonate system parameter				Function and location		
		CO_2 (μmol kg^{-1})	HCO_3^- (μmol kg^{-1})	CO_3^{2-} (μmol kg^{-1})	pH_f			
Gene	Full name	<10	<1000	<50	7.5→8.5	Putative function	Possible location – experimentally or by analogy	Predicted location by WoLF PSORT (Horton *et al.*, 2007)
AEL1	Anion exchanger like 1	↑5.5	↑5.5	↑5.5	–	HCO_3^- transport, probably coupled to Na^+, Cl^- and/or H^+ transport	Plasma membrane or chloroplast. A diatom homolog has been shown to be plasma membrane-located (Nakajima *et al.*, 2013)	Plasma membrane
αCA1	α carbonic anhydrase 1	↑10.8	↑10.8	↑10.8	–	$HCO_3^- + H^+ \leftrightarrow CO_2 + H_2O$	αCAs are distributed throughout all kingdoms of life. In *Chlamydomonas* they are found in the periplasmic space and the thylakoid lumen (Spalding, 2008). In the diatoms *Phaeodactylum tricornutum* and *Thalassiosira pseudonana*, putative αCAs were located in the four layered plastid membrane system and inside the chloroplast, respectively (Tachibana *et al.*, 2011)	Nucleus, cytosol
αCA2	α carbonic anhydrase 2	–	–	–	–	$HCO_3^- + H^+ \leftrightarrow CO_2 + H_2O$		Nucleus
βCA	β carbonic anhydrase	[a]↑454.7	[a]↑454.7	[a]↑454.7	–	$HCO_3^- + H^+ \leftrightarrow CO_2 + H_2O$	Plastid. Two βCAs have been localized to the stroma/pyrenoid in the diatom *P. tricornutum* (Tachibana *et al.*, 2011)	Chloroplast
γCA	γ carbonic anhydrase	–	–	–	–	$HCO_3^- + H^+ \leftrightarrow CO_2 + H_2O$ [b] (Soto *et al.*, 2006)	Mitochondrial location in Arabidopsis and *P. tricornutum*. γ-type CAs are found in the cyanobacteria carboxysome	Cytosol
δCA	δ carbonic anhydrase	↑9.2	↑9.2	↑9.2	–	$HCO_3^- + H^+ \leftrightarrow CO_2 + H_2O$ [b] (Soto *et al.*, 2006)	Plasma membrane location based on dinoflagellate δCAs (Lapointe *et al.*, 2008)	Plasma membrane
RubisCO	RubisCO	↑5.3	↑5.3	↑5.3	–	Carbon fixation	Chloroplast	Chloroplast
HVCN1	Voltage-gated H^+ channel	–	–	–	–	H^+ channel [b](Taylor *et al.*, 2011)	Plasma membrane (Taylor *et al.*, 2011)	Cytosol
ATPVc'/c	Vacuolar-type H^+ pump	↑4.4	↑4.4	↑4.4	–	Vacuolar-type ATP driven H^+ pump [b](Corstjens *et al.*, 2001)	Endomembrane system, possibly CV-associated membrane fraction (Corstjens *et al.*, 2001)	Vacuole
PATP	Plasma membrane type H^+ pump	↑7.1	↑7.1	↑7.1	–	'PM'-type ATP driven H^+ pump	Plasma membrane	Plasma membrane
CAX3	Ca^{2+}/H^+ exchanger 3	↑4.4	↑4.4	↑4.4	–	Ca^{2+}/H^+ exchanger – driven by a H^+ gradient	Endomembrane based on plant and yeast CAX proteins	Cytosol
NhaA2	Na^+/H^+ exchanger 2	↑4.9	↑4.9	↑4.9	–	Na^+/H^+ exchanger – maintains cellular pH and membrane potential	–	Nucleus, cytosol
LCIX	Low CO_2 induced gene	↑189.3	↑189.3	↑189.3	–	Putative low CO_2 induced gene found in *Chlamydomonas*	Chloroplast but no transmembrane regions	Nucleus
AQP2	Aquaporin 2	–	–	–	–	H_2O-permeable channel. Some are CO_2 permeable.	–	Plasma membrane
GPA	Glutamic acid, proline, alanine rich protein	↑11	↑11	↑11	–	Ca^{2+} binding protein [b] (Corstjens *et al.*, 1998)	Coccolith vesicle?	Nucleus

Arrows indicate a significant up-regulation ($P < 0.05$) of the investigated genes at low CO_2 (< 10 μmol kg^{-1}), HCO_3^- (< 1000 μmol kg^{-1}), and CO_3^{2-} (< 50 μmol kg^{-1}), compared with the lowest measured expression at high dissolved inorganic carbon (DIC) (> *c.* 1000 μmol kg^{-1}). Numbers behind arrows denote the maximum fold change that has been observed. Shading indicates a consistent up-regulation with decreasing levels of the respective carbonate system parameter (see Fig. 4).
[a]No statistical evaluation was possible because some replicates were below the detection limit.
[b]Indicates partially characterized in coccolithophores.

Shapiro–Wilk's test ($P = 0.05$). Nonnormally distributed subsets were Box–Cox-transformed. Subsets that remained nonnormally distributed were analyzed with the PERMANOVA.

ANOVA: The difference of individual treatments within an experiment was tested with Tukey's HSD *post-hoc* test (P values from *post-hoc* tests are denoted by $P_{\text{post hoc}}$). Homogeneity of variance was tested using Levene's test and was accepted if the P-value was > 0.05. Where P was smaller, the significance level (P-value of the ANOVA and the *post-hoc* test) was decreased to 0.01. Subsets treated this way are marked in Table S2.

PERMANOVA: A resemblance matrix was created using the Euclidian distance function and further processed with a one-factorial PERMANOVA design choosing type III partitioning of the sum of squares. In cases where statistically significant differences were detected, a pairwise comparison of treatments (analog to a *post-hoc* test) was conducted in a second PERMANOVA run. The numbers of permutations for each run are given in Table S2. In pairwise PERMANOVA runs, these numbers were not sufficiently high (< 100) to get reasonable results for P, so that an additional Monte Carlo test was conducted. Significance levels of the PERMANOVA analysis are the same as for the ANOVA, but by convention are termed P(perm) for the permutation P-value and $P_{\text{post hoc}}$(MC) for the Monte Carlo P-value to distinguish them.

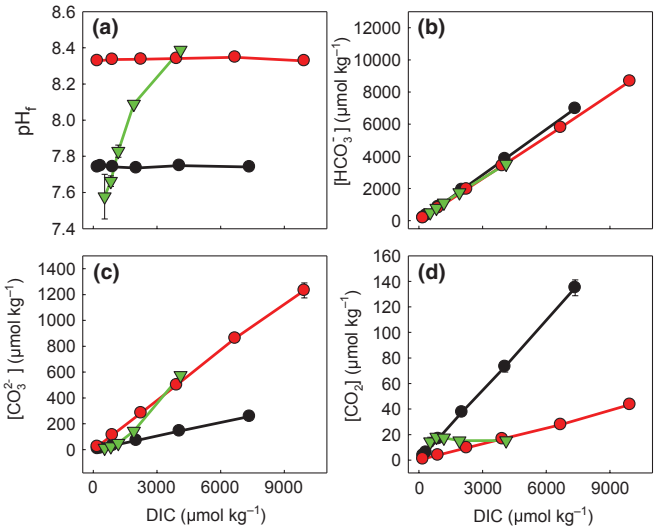

Fig. 1 Physiologically relevant carbonate chemistry parameters in relation to dissolved inorganic carbon (DIC). (a) pH_f. (b) $[HCO_3^-]$. (c) $[CO_3^{2-}]$. (d) $[CO_2]$. Error bars account for the mean change (mean of triplicates) of the particular carbonate chemistry parameter over the course of the experiments. Black circles, constant $pH_f = 7.74$; red circles, constant $pH_f = 8.34$; triangles, constant CO_2. Note that error bars are in most cases masked by symbol size.

Results

Growth and POC production rates are sensitive to low CO_2 (and HCO_3^-) and to low pH, but not to elevated CO_2

To determine the importance of individual components of the carbonate system for *E. huxleyi* physiology, cells were grown in three separate experiments at constant pH_f (7.74 and 8.34) and constant CO_2 (16 μmol kg^{-1}). Fig. 1 shows how the carbonate system changed within the three experiments. By maintaining relatively low cell concentrations, changes in carbonate chemistry as a result of biological processes were kept to a minimum over the time of the experiments. This is indicated by the error bars in Fig. 1 with the corresponding values in Table S3.

Within the ranges examined, growth and POC production rates were primarily influenced by changes in carbonate chemistry from low to intermediate HCO_3^- (160–2000 μmol kg^{-1}) and CO_2 (0.8–20 μmol kg^{-1}) (Fig. 2) with neither pH nor CO_3^{2-} having a pronounced influence (Fig. S1). Growth rates increased in all experiments with increasing concentrations of HCO_3^- and CO_2 until reaching maximum rates of *c.* 1.1 d^{-1} where further CO_2 or HCO_3^- increases had no effect on growth rates. The constant-pH experiments allow us to differentiate between the effects of CO_2 and HCO_3^- on growth rate. CO_2 demonstrates a good correlation with growth rate in both constant-pH experiments, whereas the influence of HCO_3^- on growth rate is more variable (Fig. 2a,b), suggesting that CO_2 is the principal factor responsible for growth inhibition below a $[CO_2]$ of *c.* 7.5 μmol kg^{-1} (Fig. 2b). No effect of pH on growth rate was observed in the constant-pH treatments (7.74 and 8.34). However, at constant CO_2, growth rates are significantly lower at pH 7.58 than at pH 7.83 ($P_{post\text{-}hoc} = 0.009$), which cannot be explained by a decrease in $[CO_2]$ or $[HCO_3^-]$ (Fig. 2a,b). Thus, below pH_f 7.74, $[H^+]$ appears to have a direct negative influence on growth rate.

Particulate organic carbon production rates in both constant-pH experiments were highly sensitive to HCO_3^- and CO_2 when the concentrations dropped below *c.* 2000 and 10 μmol kg^{-1}, respectively (Fig. 2c,d). The rates appear to correlate best to CO_2 at concentrations $<$ *c.* 5 μmol kg^{-1}, although there are limited data points in this range. At a constant CO_2, the lowest HCO_3^- treatment also showed significantly lower POC production rates than at intermediate HCO_3^- ($P_{\text{post hoc}} = 0.002$, Fig. 2c). At HCO_3^- concentrations $>$ *c.* 2000 μmol kg^{-1} POC production rates display a slight but significant decrease of *c.* 20% at a constant pH_f of 8.34 and 10% at a constant pH_f of 7.74 up to the highest HCO_3^- concentrations (Fig. 2c; pH 8.34, $P_{\text{post hoc}} < 0.001$; pH 7.74, $P_{\text{post hoc}}$ (MC) = 0.004). In summary, POC production showed no clear overall correlation with any of the carbonate chemistry parameters, but appears to be driven by CO_2 in the very low CO_2 range ($<$ *c.* 5 μmol kg^{-1}) and decreased by HCO_3^- at concentrations $>$ 2000 μmol kg^{-1}.

At low DIC, C : N ratios decreased significantly in the constant-pH experiments, which appear to be driven primarily by a reduction in CO_2 (Table S2). This is supported by no significant changes at constant CO_2 (Table S2). Differences in C : N between treatments probably reflect variable cellular amounts of nitrogen-free relative to nitrogen-rich organic compounds. As 40–60% of the total cellular carbon in *E. huxleyi* is in the form of lipids (Fernandez *et al.*, 1994), the decrease in C : N is likely to reflect reduced assimilation of lipids and polysaccharides at low DIC.

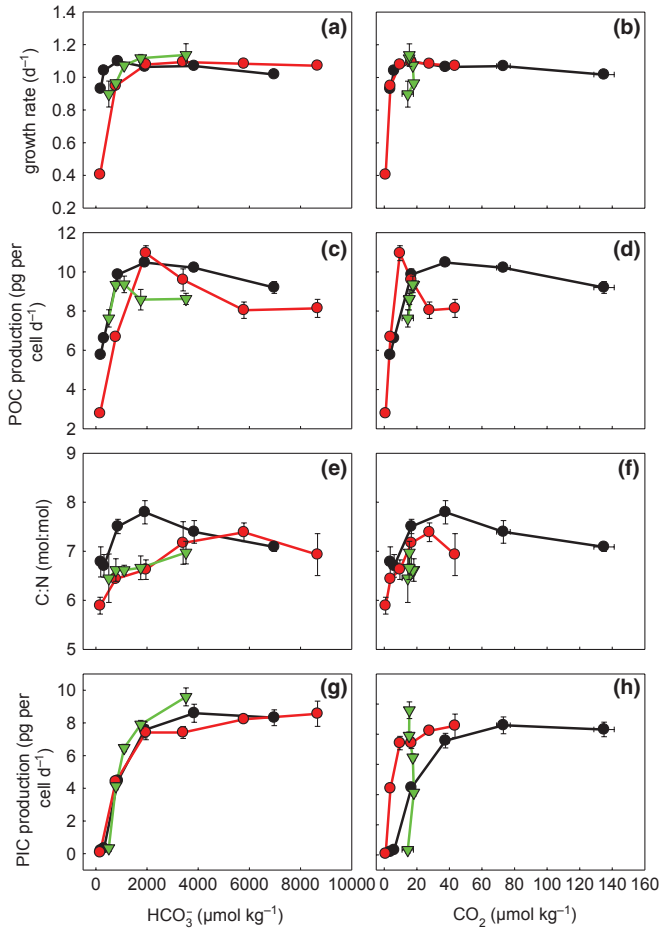

Fig. 2 Physiological response parameters for *Emiliania huxleyi* in relation to [HCO_3^-] (left column) and [CO_2] (right column). (a, b) Growth rates; (c, d) particulate organic carbon (POC) production; (e, f) C : N ratio; (g, h) particulate inorganic carbon (PIC) production. Black circles, constant pH_f = 7.74; red circles, constant pH_f = 8.34; triangles, constant CO_2. Vertical error bars denote the standard deviation of three replicates. Horizontal error bars show the mean change in [HCO_3^-] or [CO_2] (mean of triplicates) from the beginning to the end of the experiments.

Calcification is primarily driven by HCO_3^- and does not act as a CCM

Calcification rates (PIC production) increased similarly in all experiments with increasing [HCO_3^-] (Fig. 2g). Maximum calcification rates at constant pH_f values of 8.34 and 7.74 were identical, but were reached at lower CO_2 and higher CO_3^{2-} at a constant pH_f of 8.34, indicating that calcification is not primarily dependent on [CO_2] or [CO_3^{2-}] (Figs 2h, S1h). A limited control of calcification by [CO_2] is further supported by the decrease in calcification rates found in the constant-CO_2 experiment. Here, calcification rates would have to remain constant if [CO_2] were of primary importance. No signs of calcification could be found in the two lowest HCO_3^- treatments at a constant pH_f of 7.74 and in two replicates of the lowest HCO_3^- treatment at constant CO_2 (Table 2). In these treatments, calcite saturation ($\Omega_{calcite}$) is < 0.31, so post-production dissolution could potentially have taken place. However, cross-polarized light microscopy and scanning electron microscopy show the absence of internal coccoliths under these conditions, indicating that the production of coccoliths is inhibited (Bach *et al.*, 2012).

Low DIC therefore results in a decrease in growth rate and POC production as well as in calcification (Figs 2, S2). However, PIC production appears to be the most sensitive to low DIC, with low calcification rates observed in several low-DIC conditions where there was no appreciable effect on POC production and growth rate (Fig. S2). This indicates that POC production is prioritized over PIC production under Ci limitation (Fig. S2), and suggests that reducing calcification rate may enable cellular resources (such as those relating to HCO_3^- uptake) to be used for photosynthesis. Calcification is clearly not operating as a CCM at low DIC, as in this case we would expect a stimulation of calcification at low DIC.

At a genetic level, the CCM is up-regulated only at low CO_2 and is not induced at current ocean CO_2 concentrations

In order to identify the molecular basis of the physiological response of *E. huxleyi* to the individual carbonate system parameters, 15 genes with putative roles in carbon transport, pH homeostasis and biomineralization were chosen for investigation (Table S1). The measurement of relative transcript abundance was chosen as the most suitable approach to allow the expression profiles of multiple genes to be accurately determined. Although transcript abundance is not a direct measurement of protein abundance or activity, it gives a good insight into the cellular demand for specific proteins and provides a strong foundation for the further characterization of genes related to a particular cellular process. All genes are normalized to three endogenous reference genes (ERGs; *ACTIN*, *α-TUBULIN* and *EFG1-α*) with

Table 2 Presence or absence of *Emiliania huxleyi* coccoliths from SEM investigations

Experiment	HCO_3^- (μmol kg^{-1})	H^+ (nmol kg^{-1})	Coccoliths found?
Constant pH_f = 7.74	200	18.2	No
	160	18.2	No
	200	18.2	No
	300	17.8	No
	330	17.8	No
	320	17.8	No
Constant pH_f = 8.34	170	4.8	Yes
	160	4.7	Yes
	170	4.7	Yes
Constant CO_2	520	30.9	No
	510	26.3	No
	490	22.9	Yes[a]

Table showing SEM analysis of individual replicates of treatments where particulate inorganic carbon (PIC) production was < 0.5 pg per cell d^{-1}. Note that coccoliths were found in all treatments and replicates not listed in this table.

[a]Cell concentrations were higher in this replicate at the end of the experiment (76 000 compared with 36 000 cell ml^{-1} in first replicate). This caused a stronger decrease in [HCO_3^-] and [H^+].

Table 3 Assumptions within the conceptual model for inorganic carbon uptake in *Emiliania huxleyi*

Assumption	Basis of assumption	Reference
Cellular organelle location and approximate relative sizes	Transmission electron micrographs	M. A. Gutowska *et al.* (unpublished)
CO_2 principal external inorganic carbon source for photosynthesis	^{14}C labeling studies; membrane inlet mass spectrometry measurements	Sikes *et al.* (1980); Schulz *et al.* (2007)
Increasing HCO_3^- over CO_2 usage for photosynthesis at low CO_2	Membrane inlet mass spectrometry identifies increasing HCO_3^- : CO_2 uptake ratio for cells acclimated to low-CO_2 conditions; up-regulation of AEL1 at low CO_2	Rost *et al.* (2003); this study
HCO_3^- pool and dual function of AEL1 in calcification and carbon-concentrating mechanism (CCM)	AEL1 previously shown to have a role in calcification; up-regulation at low dissolved inorganic carbon (DIC)	Mackinder *et al.* (2011); this study
Up-regulation of carbonic anhydrases (CAs) at low DIC	Three out of five investigated CAs showed an up-regulation in expression at low DIC	This study
Location of δCA at plasma membrane	Presence of a putative membrane anchor; localization of a dinoflagellate δCA to the plasma membrane; strong up-regulation at low CO_2 has also been demonstrated in TWCA1, a δCA from *Thalassiosira weissflogii*; up-regulation at low DIC	Soto *et al.* (2006); Lapointe *et al.* (2008); McGinn & Morel (2008); this study
Up-regulation of extracellular CA at low DIC	Increased extracellular CA activity at low DIC/high pH; up-regulation of δCA at low DIC	Nimer *et al.* (1997); this study
Localization of βCA to the chloroplast	Two βCAs from diatoms have been shown to localize to the chloroplast – specifically the pyrenoid; CA activity in the stroma chloroplast fraction of the coccolithophore *Pleurochrysis* sp.	Kitao *et al.* (2008) and Tachibana *et al.* (2011); Quiroga & González (1993)
Probable absence of cytosolic CA	Cytosolic acidification at high HCO_3^- – presence of CA would result in rapid buffering; expression of a human CA in the cytoplasm of cyanobacteria resulted in a high CO_2-requiring phenotype; cytosolic CA would increase cytosolic CO_2, leading to increased leakage at low external CO_2	Suffrian *et al.* (2011); Price & Badger (1989); this study
Switching off of calcification at low DIC to increase DIC availability for photosynthesis	The decrease in calcification before a reduction in particulate organic carbon (POC) and growth rates. The complete termination of calcification at low DIC and pH_f	This study
HCO_3^- is the principal substrate for calcification	Previous ^{14}C labeling studies; strong correlation of calcification with HCO_3^- concentration	Sikes *et al.* (1980) and Nimer *et al.* (1997); Buitenhuis *et al.* (1999) and this study
The use of pH gradients within the CCM	Up-regulation of putative H^+ transporters at low DIC	Raven (1997); this study
Increase in RubisCO	Up-regulation of RubisCO to compensate for its decrease in efficiency as a result of an increased oxygenase : carboxylase ratio at low CO_2	This study

expression plotted relative to the lowest expression level, which is set to one.

Plotting gene expression against DIC indicates the transcriptional response to changes in total DIC (Fig. 3, Table S3). Out of the 15 genes investigated, 11 showed a marked increase in expression when the cells became DIC-limited (DIC $< 1000\ \mu mol\ kg^{-1}$) but showed no repression above this concentration. This corresponds to $[CO_2]$ and $[HCO_3^-]$ thresholds of *c.* 7.5 and 800 $\mu mol\ kg^{-1}$, respectively, below which CCM gene up-regulation occurs (Fig. 4a,b). Both of these values are approximately half that of average current oceanic values (i.e. similar to pre-industrial values), suggesting that the *E. huxleyi* CCM, at least in this strain, is actually only induced at DIC concentrations lower than ambient.

Of the selected genes with putative roles in DIC transport, *AEL1* (anion exchanger like 1, belonging to the solute carrier 4 (SLC4) family), *αCA1* (alpha-carbonic anhydrase 1), *δCA* (delta-carbonic anhydrase 1) and *rubisco* (RubisCO large subunit) showed a significant DIC limited up-regulation between four and 11-fold (Table 1, Fig. 3a). Two genes, *βCA* and *LCIX* (low CO_2 induced gene X), had a large response at low DIC, with a respective 450- and 180-fold up-regulation at the lowest DIC

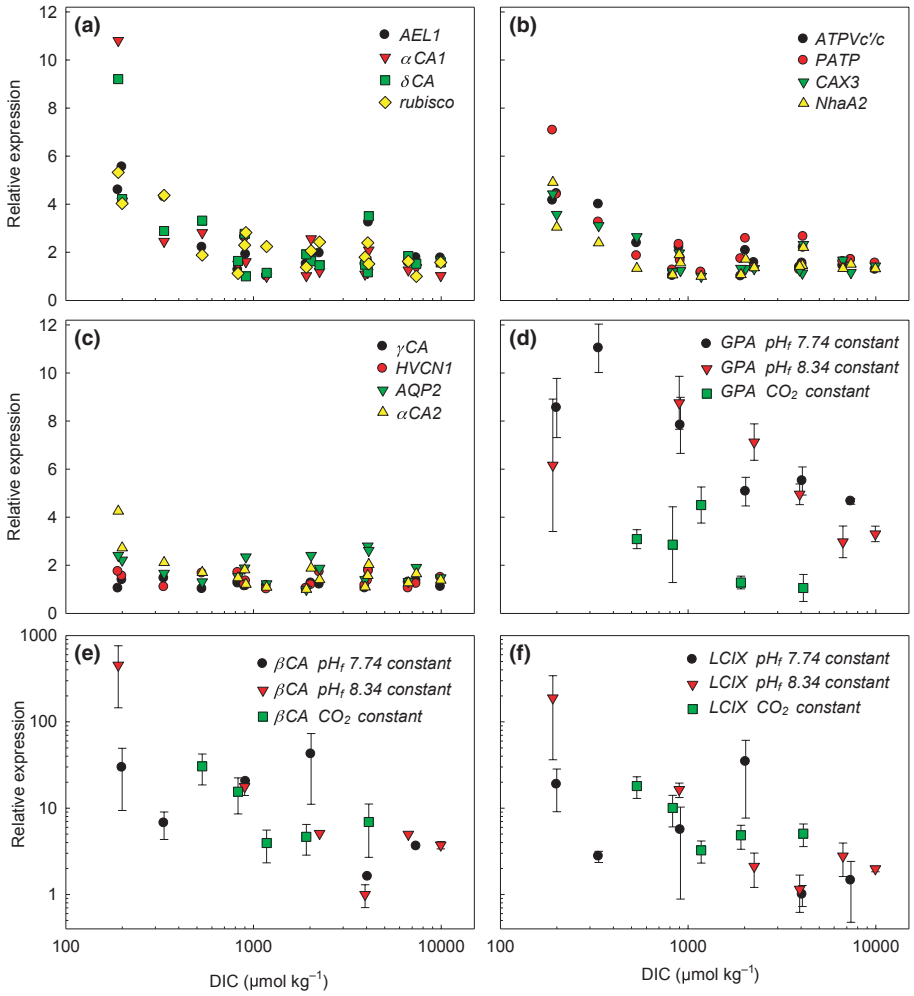

Fig. 3 Relative expression of investigated *Emiliania huxleyi* genes plotted against dissolved inorganic carbon (DIC). (a, b) Inorganic carbon transport and H^+ transport genes that were significantly up-regulated ($P < 0.05$) at DIC < *c.* 200 μmol kg^{-1} relative to DIC > 1000 μmol kg^{-1}. Panel (c) shows nonresponsive genes ($P > 0.05$) over the DIC ranges tested. Panels (a)–(c) are combined data from the constant pH_f 7.74, constant pH_f 8.34 and constant CO_2 experiments for each gene. Error bars have been omitted to improve clarity but standard deviations are listed in Table S3. Plots in (d)–(f) show expression of *GPA*, *βCA*, and *LCIX* in the three individual experiments with standard errors shown. Note the logarithmic *y*-axis for plots in (e) and (f). The absence of error bars for some samples in (e) is the result of undetectable abundances of *βCA* transcripts in some of the biological replicates. (d) shows *GPA*, which was significantly down-regulated at high (> 2000 μmol kg^{-1}) DIC compared with low (< 400 μmol kg^{-1}) DIC. Note that fold changes and corresponding significances are shown in Tables 1 and S2. *AEL1*, anion exchanger like 1; *αCA1*, alpha-carbonic anhydrase 1; *δCA*, delta-carbonic anhydrase 1; *rubisco*, RubisCO large subunit; *CAX3*, Ca^{2+}/H^+ exchanger 3; *NhaA2*, Na^+/H^+ exchanger 2; *ATPVc'/c*, vaculoar-type H^+ pump; *PATP*, plasma membrane-type H^+ pump; *HVCN1*, H^+ channel; *AQP2*, aquaporin 2; *αCA2*, alpha-carbonic anhydrase 2; *γCA*, gamma-carbonic anhydrase; *βCA*, beta-carbonic anhydrase; *LCIX*, low CO_2 induced gene X.

value in the constant-pH_f (= 8.34) experiment relative to the treatment with the lowest expression (Table 1, Fig. 3e,f). *βCA* encodes a putative carbonic anhydrase responsible for catalyzing the interconversion of CO_2 and HCO_3^-, whereas LCIX exhibits similarity to the *Chlamydomonas* LCIB protein, which is located in the chloroplast and plays a crucial role in HCO_3^- uptake (Miura *et al.*, 2004; Wang & Spalding, 2006). Furthermore, *βCA* showed a highly correlated expression with *LCIX* ($R^2 > 0.99$, data not shown), indicating that these genes could be under the same transcriptional control.

Of the putative H^+ transport-related genes, *CAX3* (Ca^{2+}/H^+ exchanger 3), *NhaA2* (Na^+/H^+ exchanger 2), *ATPVc'/c* (vaculoar-type H^+ pump) and *PATP* (plasma membrane-type H^+ pump) showed a 4–7.5 fold up-regulation (Table 1, Fig. 3b). Four genes with potential roles in H^+ and DIC transport, *HVCN1* (H^+ channel), *AQP2* (aquaporin 2), *αCA2* (alpha-carbonic anhydrase 2), and *γCA* (gamma-carbonic anhydrase), showed no significant transcriptional response over the carbonate system range tested (Fig. 3c; Table S2). Above 1000 μmol kg^{-1}, DIC changes in gene expression of most investigated genes was minimal with no repression of DIC-responsive genes, but a small but significant decrease ($P_{post\ hoc} = 0.02$) seen in GPA expression > *c.* 2000 μmol kg^{-1} (Fig. 3d).

The CCM is responsive to CO_2 and HCO_3^- but not to pH

An understanding of the regulation of the *E. huxleyi* CCM may provide important information about its mode of operation and cellular function. An examination of the individual carbonate system parameters indicated that the expression of these genes correlates closely with [CO_2] and [HCO_3^-] at low DIC (Fig. 4a,b). This indicates that although pH and CO_3^{2-} may have a synergistic effect with other factors on the expression of some genes, they do not appear to be the main parameters of the carbonate system driving the genetic responses (Fig. 4c,d). Table 1 summarizes the responses of the investigated genes along with their putative or confirmed function and potential cellular locations.

Transcriptional response to reduced calcification

Previously we demonstrated that the expression of several genes with putative roles in DIC, Ca^{2+} and H^+ transport (*AEL1*, *CAX3* and *ATPVc'/c*) show a close correlation with calcification rate, suggesting that these genes play a direct role in the calcification process (Mackinder *et al.*, 2011). When calcification was inhibited by the removal of Ca^{2+}, the expression of these calcification-associated genes was strongly repressed (Mackinder *et al.*, 2011).

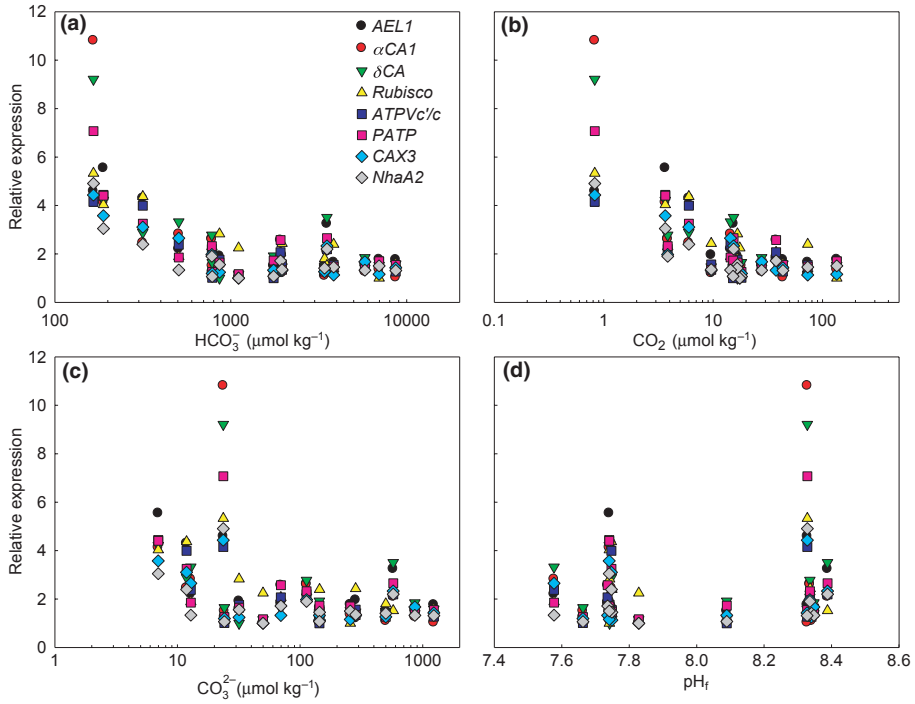

Fig. 4 Plots of *Emiliania huxleyi* gene expression vs the individual components of the carbonate system for eight dissolved inorganic carbon (DIC)-responsive genes. Error bars have been omitted to improve clarity, but standard deviations are listed in Table S1: (a) vs. HCO_3; (b) vs CO_2; (c) vs CO_3; (d) vs pH_f. *AEL1*, anion exchanger like 1; *αCA1*, alpha-carbonic anhydrase 1; *δCA*, delta-carbonic anhydrase 1; *rubisco*, RubisCO large subunit; *ATPVc'/c*, vaculoar-type H^+ pump; *PATP*, plasma membrane-type H^+ pump; *CAX3*, Ca^{2+}/H^+ exchanger 3; *NhaA2*, Na^+/H^+ exchanger 2.

However, in the present study, these genes were all induced at low DIC (Fig. 3), whereas calcification was inhibited. This indicates that these genes may play a dual role within the cell, supporting calcification under ambient conditons but switching to support photosynthesis when DIC becomes limiting.

Discussion

Growth and calcification responses to the carbonate system

The predicted changes in the ocean's carbonate system caused by increasing atmospheric CO_2 may have multiple impacts on coccolithophore physiology (Riebesell & Tortell, 2011). Using experimental manipulation of the carbonate system, we show that individual aspects of *E. huxleyi* physiology can be attributed to separate components of the carbonate system.

Growth rates presented in this study correlate closely to $[CO_2]$ (Fig. 2a), with pH_f having a significant negative impact below values of *c.* 7.7 (Fig. S1a). Although POC production does not show such a clear coupling to $[CO_2]$ as growth rates (Fig. 2d), it also responds negatively to pH_f when it drops below *c.* 7.7. A similar regulation of pH and CO_2 on growth and POC production was also seen in Bach *et al.* (2011) with a linear decrease from a pH_f of *c.* 7.7–7.0 and CO_2 dependence above a pH_f of 7.7. However, a study by Buitenhuis *et al.* (1999) saw no clear tightly coupled correlation between *E. huxleyi* growth rate and $[CO_2]$. Instead, the authors suggested that both CO_2 and HCO_3^- are important for growth rates. The reason behind this discrepancy is unclear, although it should be kept in mind that threshold values for individual carbonate system components may differ between strains and may be modulated by light conditions (Langer *et al.*, 2009; Rokitta & Rost, 2012).

Calcification rates are tightly coupled to $[HCO_3^-]$ (Fig. 2g), suggesting that HCO_3^- is the primary carbon source used for $CaCO_3$ precipitation in *E. huxleyi*. This is in agreement with previous studies (reviewed in Paasche, 2001). Simulated ocean acidification has been shown to affect coccolithophore calcification mostly negatively (Riebesell & Tortell, 2011). By comparing ocean acidification with constant-pH experiments, Bach *et al.* (2011) showed that it is the increase in H^+ at elevated CO_2 that negatively affects calcification rates of *E. huxleyi*. It is also known that intracellular pH in coccolithophores is particularly sensitive to changes in external pH (Suffrian *et al.*, 2011; Taylor *et al.*, 2011). Under these considerations, it could be expected that calcification rates would remain consistently lower throughout the constant $pH_f = 7.74$ experiment compared with the constant $pH_f = 8.34$ experiment. Surprisingly, however, this is not the case. Instead, maximum calcification rates are similar in both constant-pH experiments (Fig. 2g,h). This indicates that the direct negative effect of high $[H^+]$ on calcification rates may at some point be overcome by increasing availability of HCO_3^- substrate. This is further supported by our finding that higher $[HCO_3^-]$ was necessary to initiate calcification when $[H^+]$ in the seawater medium was higher (Table 2). Considering carbonate chemistry conditions of the past, this might provide a further explanation as to why coccolithophores were able to thrive in the early Mesozoic era, a time that was characterized by relatively low sea water pH (as low as pH 7.7) and high DIC substrate (up to 5000 μmol kg^{-1}; Ridgwell, 2005).

The nature and regulation of the CCM

Previous mass spectrometrically based work by Rost *et al.* (2003) showed that *E. huxleyi* operates a regulated CCM but gave no

indication of the mechanism. Our results support the presence of a regulated CCM and furthermore have identified several of its molecular components, the carbonate species to which it responds, the threshold at which it is induced, and its possible interactions with calcification.

The transcriptional data identify the genetic basis of a CCM in *E. huxleyi* with a clear up-regulation in multiple putative CCM-related genes as DIC becomes limiting for growth, POC and PIC production (Fig. 3, Table 1). The majority of genes were up-regulated when HCO_3^- or CO_2 dropped below *c.* 800 and 7.5 μmol kg^{-1}, respectively. Interestingly, most of the DIC-responsive genes were not further repressed at CO_2 > *c.* 7.5 μmol kg^{-1} ([HCO_3^-] *c.* 800 μmol kg^{-1}); this indicates a potential basal level of the CCM, with a low amount of active DIC transport taking place even when growth rates and POC production are saturated. The presence of active transport at ambient CO_2 and HCO_3^- is supported by Schulz *et al.* (2007), who showed active DIC uptake even at ambient conditions.

Photosynthetic O_2 evolution curves and ^{14}C incorporation studies have indicated that photosynthesis is not saturated at ambient CO_2 (Paasche, 1964; Herfort *et al.*, 2002; Rost *et al.*, 2003). This is not supported by our data with growth rates and organic carbon fixation both saturated at or below ambient [CO_2]. However, these differences could theoretically be attributed to the different light intensities used between the studies and to the fact that O_2 evolution is a measurement of photosystem II activity, not a direct measurement of CO_2 fixation. Furthermore, these thresholds may vary between strains, as seen with strain-specific responses in calcification and growth to changing carbonate chemistry (Langer *et al.*, 2009). These responses do not necessarily indicate that the underlying cellular mechanisms differ between strains, but most likely highlight differences in the regulation of cellular processes, such as calcification. This is further supported by an optimum curve response, with different strains and species having varying optimum calcification rates in relation to pCO_2, but the overall response (i.e. the shape of the curve) being very similar (Langer *et al.*, 2006, 2009; Ridgwell *et al.*, 2009; Bach *et al.*, 2011; Krug *et al.*, 2011). However, a greater understanding at the molecular level of the response of different *E. huxleyi* strains and coccolithophore species to changes in carbonate chemistry is critical to extrapolate our data to other coccolithophores.

The CCM of *E. huxleyi* shows a number of differences from those of other partially characterized eukaryotic algae. One outstanding feature is its low affinity for CO_2 (Rost *et al.*, 2003) with a $K_{1/2}$ for CO_2 that is several-fold higher than the $K_{1/2}$ for the prymnesiophyte *Phaeocystis globosa* and several diatom species (Johnston & Raven, 1996; Rost *et al.*, 2003; Trimborn *et al.*, 2009). Another feature of the *E. huxleyi* CCM is that up-regulation of molecular components seems to occur only when very low CO_2 concentrations are reached. This is strikingly different from diatoms and *Chlamydomonas*, where molecular CCM components are already strongly induced at ambient CO_2 and even above (Harada *et al.*, 2005; Brueggeman *et al.*, 2012).

Although the *E. huxleyi* CCM may be of a lower affinity, the basic components appear to be similar to other eukaryotic algae. CAs play fundamental roles within algal CCMs, and CAs associated with the CCM are generally up-regulated under carbon limitation (Badger, 2003; Raven & Giordano, 2009). Genome analysis shows that *E. huxleyi* has nine putative CAs belonging to the α, β, γ and δ families. This CA composition demonstrates strong similarities with *Chlamydomonas*, which has 10 putative CAs in its genome belonging to the α, β and γ families (Spalding, 2008). It is also very similar to the diatom CA repertoire, with *Phaeodactylum tricornutum* also having nine CAs distributed across the same four families (Tachibana *et al.*, 2011). Diatoms also possess multiple homologs to *AEL1*. The characterization of *P. tricornutum* SLC4-2 shows that it is induced at low CO_2, localizes to the plasma membrane and stimulates HCO_3^- uptake and photosynthesis (Nakajima *et al.*, 2013). Wolf PSORT predicts a plasma membrane location for AEL1 (Table 1) and its low HCO_3^-/CO_2-dependent expression suggests a related function in *E. huxleyi*.

Localized intracellular pH gradients and regulation are thought to be a fundamental part of CCMs (Raven, 1997). The increased expression of putative proton pumps (ATPVc′/c and PATP) and cation/H^+ exchangers (NhaA2 and CAX3) suggests an increased demand of these transporters to maintain pH homeostasis, membrane potential or alter compartmental pH in order to promote changes in $CO_2 : HCO_3^-$ ratios. More alkaline regions would maintain DIC as HCO_3^-, which is one million times less permeable to membranes than CO_2 (Moroney *et al.*, 2011). This could prevent CO_2 loss via diffusion across membranes, while more acidic regions in the proximity of RubisCO would result in a shift to CO_2 (Raven, 1997).

Although HCO_3^- use appears to become increasingly important at low DIC (Rost *et al.*, 2003; Schulz *et al.*, 2007; *AEL1* up-regulation at low DIC shown here), growth rates are ultimately determined by CO_2 (Fig. 2b). By operating a CCM, the cell actively accumulates HCO_3^- and CO_2 at a higher concentration in the proximity of RubisCO than externally. DIC has to be presented to RubisCO as CO_2, so ultimately HCO_3^- accumulated for carbon fixation will have to be converted to CO_2. If the external CO_2 concentration is very low, the diffusion gradient from the chloroplast to the outside will be large and leakage increases (Rost *et al.*, 2006). Leakage in *E. huxleyi* has been measured to be *c.* 79% at ambient CO_2 (Schulz *et al.*, 2007) and shown to increase as CO_2 decreased (Rost *et al.*, 2006). Thus, external [CO_2] largely determines how much accumulated DIC stays within the cell as a result of the strong inside-to-out CO_2 gradient and high permeability of membranes to CO_2.

Calcification as a CCM

Coccolithophores have maintained calcification since coccoliths appeared in the fossil record *c.* 220 million yr ago (Bown *et al.*, 2004). A proposed role for the maintenance of calcification in coccolithophores is to support photosynthesis by using H^+ generated by the production of calcium carbonate from bicarbonate (Paasche, 2001). Whilst carbon fixation by photosynthesis and calcification can occur at a similar rate within a cell, there is increasing evidence suggesting that the two processes are not

tightly linked. It is possible to inhibit calcification by limiting calcium (Herfort *et al.*, 2004; Trimborn *et al.*, 2007; Leonardos *et al.*, 2009) or DIC (Buitenhuis *et al.*, 1999; this study), whilst photosynthesis, growth and POC production rates remain unaffected (Trimborn *et al.*, 2007; constant-CO_2 experiment of this study). Photosynthesis therefore appears to have no mechanistic dependence on calcification (Leonardos *et al.*, 2009). Our data support this and strongly suggest that calcification does not function as a CCM at low DIC.

Moreover, our data reveal that calcification is actually inhibited at low DIC, rather than induced. Current evidence indicates that coccolithophores largely use CO_2 for photosynthesis and HCO_3^- for calcification (reviewed in Paasche, 2001), which is supported by our own observations. Thus, inhibition of calcification would enable the cell to utilize the HCO_3^- normally acquired for calcification as a substrate for photosynthesis. Here we provide the first transcriptional dataset in support of this hypothesis. We found that the expression of three putative calcification-related ion transporters was elevated under limiting DIC, whilst calcification was inhibited. For example, assuming AEL1 functions as a plasma membrane HCO_3^- transporter in *E. huxleyi*, as with SLC4-2 in diatoms, under normal conditions it most probably acts to transport HCO_3^- into an intracellular pool for calcification (Fig. 5a). This is supported by *AEL1* expression being repressed when calcification is inhibited by calcium limitation or in noncalcifying strains (Mackinder *et al.*, 2011). However, under low CO_2 and HCO_3^- availability, *AEL1* is induced, whereas calcification is inhibited. This suggests that there is an increased need for HCO_3^- transport at low DIC, but that this HCO_3^- is diverted away from the coccolith vesicle into the chloroplast for photosynthetic carbon fixation (Fig. 5b). Further functional characterization and localization of AEL1 and other CCM/calcification components is critical to validate this model and to fully understand this process at the molecular level.

Extrapolation to the real ocean

The expression data indicate an up-regulation of the CCM occurring at low DIC ([CO_2] *c.* 7.5 μmol kg^{-1}), suggesting that an inducible CCM is redundant in this *E. huxleyi* strain under current oceanic [CO_2] (*c.* 16 μmol kg^{-1}). However, in their natural habitat, it is possible that cells sporadically experience [CO_2] < 7.5 μmol kg^{-1}, in particular at the end of a bloom where [CO_2] is reduced as a result of photosynthetic carbon drawdown. Values as low as *c.* 5 μmol kg^{-1} were seen in a mesocosm experiment where an *E. huxleyi* bloom occurred after a *Phaeocystis* sp. and diatom bloom (Purdie & Finch, 1994). Furthermore, [CO_2] was significantly lower before the onset of anthropogenic CO_2 release *c.* 200 yr ago, so that limiting DIC concentrations might have occurred more frequently in the past. A third aspect, which has to be considered, is a possible variability in the threshold DIC concentration below which the CCM is up-regulated. Variable thresholds either could result from strain-specific differences between *E. huxleyi* clones (Langer *et al.*, 2009) and/or could be altered by culture conditions (Rokitta & Rost, 2012). At very high light conditions, for example, it is possible that the CCM becomes up-regulated at a higher CO_2 threshold, owing to the cell having a larger DIC demand. Finally, the necessity of an inducible CCM in *E. huxleyi* can only be reliably determined by in field experiments where regulation patterns are investigated in *in situ* conditions.

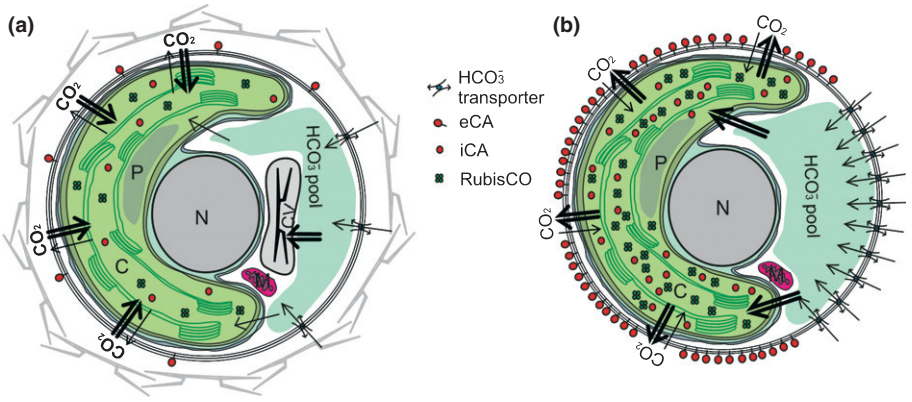

Fig. 5 A conceptual model of inorganic carbon uptake in *Emiliania huxleyi* at high (a) and low (b) dissolved inorganic carbon (DIC). The model is based on the data presented in this manuscript and previous studies (see Table 3 for all assumptions within the model). (a) With increasing CO_2, the CO_2 gradient into the cell becomes, at some point, sufficient to saturate photosynthesis and maintain maximum particulate organic carbon (POC) fixation and growth rates. Hence CO_2 is the most important external substrate for photosynthesis at high CO_2, while HCO_3^- is the main substrate for calcification with a putative HCO_3^- exchanger AEL1 playing a key role. (b) At low CO_2, HCO_3^- becomes more and more important as the inorganic carbon source for photosynthesis. Therefore, HCO_3^- and its uptake mechanism shift from providing inorganic carbon for calcification to photosynthesis, leading to a reduction and, eventually, to a deactivation of calcification. Furthermore, the carbon-concentrating mechanism (CCM) (including the components shown: RubisCO, external and internal CAs) is up-regulated to support inorganic carbon supply. Although HCO_3^- becomes the dominant external carbon source for photosynthesis, external CO_2 still strongly influences growth rates and POC fixation as a result of increasing CO_2 leakage as external CO_2 decreases (see text for details). C, chloroplast; P, pyrenoid; N, nucleus; M, mitochondrium; CV, coccolith vesicle; eCA, external carbonic anhydrase; iCA, internal carbonic anhydrase.

Increased pCO_2 has been shown to affect intracellular processes like calcification and photosynthesis in coccolithophores (Riebesell *et al.*, 2000; Langer *et al.*, 2006, 2009). In contrast to these physiological responses, our data suggest that the regulatory response to these changes at a genetic level is very limited. CO_2 and HCO_3^- only enhanced transcription of genes at concentrations significantly below those currently experienced and well below concentrations predicted in the near future. Furthermore, none of the investigated genes – even putative H^+ pumps – were responsive to increasing sea water $[H^+]$. There are two possible explanations for this lack of regulatory response: we have simply missed the critical pH and high CO_2 responsive genes; or *E. huxleyi* does indeed entirely lack a regulatory machinery to cope with ocean acidification. The former can only be addressed in similar future studies that investigate the whole transcriptome. However, if future studies support the latter then the inability to regulate to changing pH could offer an explanation as to why calcification and photosynthesis are negatively affected below certain pH thresholds.

The novel approach applied in this study has allowed us to tease out the complexities of, and interactions between, photosynthesis and calcification in the ecologically important phytoplankton, *E. huxleyi*, and their responses to changing pCO_2. The data presented provide a significant step forward in understanding the underlying cellular and molecular mechanisms of these processes, providing strong evidence that calcification does not function as a CCM and indicating that *E. huxleyi* may have evolved mechanisms to deal with limiting rather than elevated pCO_2.

Acknowledgements

Silke Lischka is acknowledged for support on statistics and Janett Voigt for support during sampling. Furthermore, we thank three anonymous reviewers for their valuable comments, which helped to improve the manuscript. The work was funded by CalMarO a FP7 Marie Curie Initial training network and the Federal Ministry of Education and Research (Bundesministerium für Bildung und Forschung; 03F0608A) in the framework of the Biological Impacts of Ocean Acidification (BIOACID) project (subproject 3.1.1).

References

Bach LT, Bauke C, Meier KJS, Riebesell U, Schulz KG. 2012. *Influence of changing carbonate chemistry on morphology and weight of coccoliths formed by Emiliania huxleyi. Biogeosciences* **9**: 3449–3463.

Bach LT, Riebesell U, Schulz KG. 2011. Distinguishing between the effects of ocean acidification and ocean carbonation in the coccolithophore *Emiliania huxleyi. Limnology and Oceanography* **56**: 2040–2050.

Badger M. 2003. The roles of carbonic anhydrases in photosynthetic CO_2 concentrating mechanisms. *Photosynthesis Research* **77**: 83–94.

Bown PR, Lees JA, Young JR. 2004. Calcareous nannoplankton evolution and diversity through time. In: Thierstein HR, Young JR, eds. *Coccolithophores – from molecular processes to global impact.* Berlin, Germany: Springer Verlag, 481–505.

Brueggeman AJ, Gangadharaiah DS, Cserhati MF, Casero D, Weeks DP, Ladunga I. 2012. Activation of the carbon concentrating mechanism by CO_2 deprivation coincides with massive transcriptional restructuring in *Chlamydomonas reinhardtii. Plant Cell* **24**: 1860–1875.

Buitenhuis E, de Baar H, Veldhuis M. 1999. Photosynthesis and calcification by *Emiliania huxleyi* (Prymnesiophyceae) as a function of inorganic carbon species. *Journal of Phycology* **35**: 949–959.

Caldeira K, Wickett ME. 2003. Anthropogenic carbon and ocean pH. *Nature* **425**: 365.

Corstjens P, Araki Y, González EL. 2001. A coccolithophorid calcifying vesicle with a vacuolar-type ATPase proton pump: cloning and immunolocalisation of the V0 subunit c1. *Journal of Phycology* **37**: 71–78.

Corstjens P, Van Der Kooij A, Linschooten C, Brouwers GJ, Westbroek P, de Vrind de Jong E. 1998. GPA, a calcium–binding protein in the coccolithophorid *Emiliania huxleyi* (Prymnesiophyceae). *Journal of Phycology* **34**: 622–630.

von Dassow P, Ogata H, Probert I, Wincker P, Da Silva C, Audic S, Claverie J-M, de Vargas C. 2009. Transcriptome analysis of functional differentiation between haploid and diploid cells of *Emiliania huxleyi*, a globally significant photosynthetic calcifying cell. *Genome Biology* **10**: R114.

Dickson AG, Afghan JD, Anderson GC. 2003. Reference materials for oceanic CO_2 analysis: a method for the certification of total alkalinity. *Marine Chemistry* **80**: 185–197.

Falkowski PG, Raven J. 2007. *Aquatic photosynthesis.* Princeton, NJ, USA: Princeton University Press.

Fernandez E, Balch WM, Maranon E, Holligan PM. 1994. High rates of lipid biosynthesis in cultured, mesocosm and coastal populations of the coccolithophore *Emiliania huxleyi. Marine Ecology Progress Series* **22**: 13–22.

Field CB, Behrenfeld MJ, Randerson JT, Falkowski P. 1998. Primary production of the biosphere: integrating terrestrial and oceanic components. *Science* **281**: 237–240.

Giordano M, Beardall J, Raven JA. 2005. CO_2 concentrating mechanisms in algae: mechanisms, environmental modulation, and evolution. *Annual Review of Plant Biology* **56**: 99–131.

Guillard R, Ryther J. 1962. Studies of marine planktonic diatoms. I. *Cyclotella nana* Hustedt, and *Detonula confervacea* (cleve) Gran. *Canadian Journal of Microbiology* **8**: 229–239.

Hansen HP, Koroleff F. 1999. Determination of nutrients. In: Grasshoff K, Kremling K, Ehrhardt M, eds. *Methods of seawater analysis, 3rd edn.* Weinheim, Germany: Wiley-VCH Verlag GmbH, 159–228.

Harada H, Nakatsuma D, Ishida M, Matsuda Y. 2005. Regulation of the expression of intracellular beta-carbonic anhydrase in response to CO_2 and light in the marine diatom *Phaeodactylum tricornutum. Plant Physiology* **139**: 1041–1050.

Herfort L, Loste E, Meldrum F, Thake B. 2004. Structural and physiological effects of calcium and magnesium in *Emiliania huxleyi* (Lohmann) Hay and Mohler. *Journal of Structural Biology* **148**: 307–314.

Herfort L, Thake B, Roberts J. 2002. Acquisition and use of bicarbonate by *Emiliania huxleyi. New Phytologist* **156**: 427–436.

Horton P, Park K-J, Obayashi T, Fujita N, Harada H, Adams-Collier CJ, Nakai K. 2007. WoLF PSORT: protein localization predictor. *Nucleic Acids Research* **35**: W585–W587.

Johnston AM, Raven JA. 1996. Inorganic carbon accumulation by the marine diatom *Phaeodactylum tricornutum. European Journal of Phycology* **31**: 285–290.

Kester DR, Duedall IW, Connors DN, Pytkowicz RM. 1967. Preparation of artificial seawater. *Limnology and Oceanography* **12**: 176–179.

Kitao Y, Harada H, Matsuda Y. 2008. Localization and targeting mechanisms of two chloroplastic beta-carbonic anhydrases in the marine diatom *Phaeodactylum tricornutum. Physiologia Plantarum* **133**: 68–77.

Krug SA, Schulz KG, Riebesell U. 2011. Effects of changes in carbonate chemistry speciation on *Coccolithus braarudii*: a discussion of coccolithophorid sensitivities. *Biogeosciences* **8**: 771–777.

Langer G, Geisen M, Baumann K-H, Kläs J, Riebesell U, Thoms S, Young JR. 2006. Species-specific responses of calcifying algae to changing seawater carbonate chemistry. *Geochemistry Geophysics Geosystems* **7**: Q09006.

Langer G, Nehrke G, Probert I, Ly J, Ziveri P. 2009. Strain-specific responses of *Emiliania huxleyi* to changing seawater carbonate chemistry. *Biogeosciences* **6**: 4361–4383.

Lapointe M, MacKenzie TDB, Morse D. 2008. An external δ-carbonic anhydrase in a free-living marine dinoflagellate may circumvent diffusion-limited carbon acquisition. *Plant Physiology* **147**: 1427–1436.

LaRoche J, Rost B, Engel A. 2010. Bioassay, batch culture and chemostat experimentation. In: Riebesell U, Fabry V, Hansson L, Gattuso JP, eds. *Guide for best practices for ocean acidification research and data reporting*: Publications Office of the European Union, 81–94.

Leonardos N, Read B, Thake B, Young JR. 2009. No mechanistic dependence of photosynthesis on calcification in the coccolithophorid *Emiliania huxleyi* (Haptophyta). *Journal of Phycology* **45**: 1046–1051.

Lewis E, Wallace DWR. 1998. *Program developed for CO_2 systems calculations*. Oak Ridge, TN, USA: ORNL/CDIAC-105 Carbon Dioxide Information Analysis Centre, Oak Ridge National Laboratory, US Department of Energy.

Mackinder L, Wheeler G, Schroeder D, von Dassow P, Riebesell U, Brownlee C. 2011. Expression of biomineralization-related ion transport genes in *Emiliania huxleyi*. *Environmental Microbiology* **13**: 3250–3265.

McGinn PJ, Morel FM. 2008. Expression and regulation of carbonic anhydrases in the marine diatom *Thalassiosira pseudonana* and in natural phytoplankton assemblages from Great Bay, New Jersey. *Physiologia Plantarum* **133**: 78–91.

Miura K, Yamano T, Yoshioka S, Kohinata T, Inoue Y, Taniguchi F, Asamizu E, Nakamura Y, Tabata S, Yamato KT, *et al.* 2004. Expression Profiling-Based Identification of CO_2-responsive genes regulated by CCM1 controlling a carbon-concentrating mechanism in *Chlamydomonas reinhardtii*. *Plant Physiology* **135**: 1595–1607.

Moore TS, Dowell MD, Franz BA. 2012. Detection of coccolithophore blooms in ocean color satellite imagery: a generalized approach for use with multiple sensors. *Remote Sensing of Environment* **117**: 249–263.

Moroney J, Ma Y, Frey W, Fusilier K, Pham T, Simms T, DiMario R, Yang J, Mukherjee B. 2011. The carbonic anhydrase isoforms of *Chlamydomonas reinhardtii*: intracellular location, expression, and physiological roles. *Photosynthesis Research* **109**: 133–149.

Nakajima K, Tanaka A, Matsuda Y. 2013. SLC4 family transporters in a marine diatom directly pump bicarbonate from seawater. *Proceedings of the National Academy of Sciences, USA* **110**: 1767–1772.

Nimer NA, IglesiasRodriguez MD, Merrett MJ. 1997. Bicarbonate utilization by marine phytoplankton species. *Journal of Phycology* **33**: 625–631.

Nimer NA, Merrett MJ. 1992. Calcification and utilization of inorganic carbon by the coccolithophorid *Emiliania huxleyi* Lohmann. *New Phytologist* **121**: 173–177.

Paasche E. 1964. A tracer study of the inorganic carbon uptake during coccolith formation and photosynthesis in the coccolithophorid *Coccolithus huxleyi*. *Physiologia Plantarum Supplementum* **3**: 1–82.

Paasche E. 2001. A review of the coccolithophorid *Emiliania huxleyi* (Prymnesiophyceae), with particular reference to growth, coccolith formation, and calcification-photosynthesis interactions. *Phycologia* **40**: 503–529.

Poulton AJ, Adey TR, Balch WM, Holligan PM. 2007. Relating coccolithophore calcification rates to phytoplankton community dynamics: regional differences and implications for carbon export. *Deep Sea Research Part II* **54**: 538–557.

Price GD, Badger MR. 1989. Expression of human carbonic anhydrase in the cyanobacterium *Synecoccus* PCC 7942 creates a high CO_2-requiring phenotype. *Plant Physiology* **91**: 505–513.

Purdie DA, Finch MS. 1994. Impact of a coccolithophorid bloom on dissolved carbon dioxide in sea water enclosures in a Norwegian fjord. *Sarsia* **79**: 379–387.

Quiroga O, González EL. 1993. Carbonic anhydrase in the chloroplast of a coccolithophorid (Prymnesiophyceae). *Journal of Phycology* **29**: 321–324.

Raven J. 1997. Putting the C in phycology. *European Journal of Phycology* **32**: 319–333.

Raven JA, Giordano M. 2009. Biomineralization by photosynthetic organisms: evidence of coevolution of the organisms and their environment? *Geobiology* **7**: 140–154.

Reinfelder JR. 2011. Carbon concentrating mechanisms in eukaryotic marine phytoplankton. *Annual Review of Marine Science* **3**: 291–315.

Ridgwell A. 2005. A Mid Mesozoic revolution in the regulation of ocean chemistry. *Marine Geology* **217**: 339–357.

Ridgwell A, Schmidt DN, Turley C, Brownlee C, Maldonado MT, Tortell P, Young JR. 2009. From laboratory manipulations to earth system models: predicting pelagic calcification and its consequences. *Biogeosciences Discussions* **6**: 3455–3480.

Riebesell U, Tortell PD. 2011. Effects of ocean acidification on pelagic organisms and ecosystems. In: Gattuso JP, Hansson L, eds. *Ocean acidification*. Oxford, UK: Oxford University Press, 99–121.

Riebesell U, Zondervan I, Rost B, Tortell PD, Zeebe RE, Morel FMM. 2000. Reduced calcification of marine plankton in response to increased atmospheric CO_2. *Nature* **407**: 364–367.

Rokitta SD, Rost B. 2012. Effects of CO_2 and their modulation by light in the life-cycle stages of the coccolithophore *Emiliania huxleyi*. *Limnology & Oceanography* **57**: 607–618.

Rost B, Riebesell U, Burkhardt S, Sültemeyer D. 2003. Carbon acquisition of bloom-forming marine phytoplankton. *Limnology and Oceanography* **48**: 55–67.

Rost B, Riebesell U, Sültemeyer D. 2006. Carbon acquisition of marine phytoplankton: effect of photoperiod length. *Limnology and Oceanography* **51**: 12–20.

Roy RN, Roy LN, Vogel KM, Porter-Moore C, Pearson T, Good CE, Millero FJ, Campbell DM. 1993. The dissociation constants of carbonic acid in seawater at salinities 5 to 45 and temperatures 0 to 45°C. *Marine Chemistry* **44**: 249–267.

Sarmiento J, Gruber N. 2006. *Ocean biogeochemical dynamics*. Princeton, NJ, USA: Princeton University Press.

Schulz KG, Rost B, Burkhardt S, Riebesell U, Thoms S, Wolf-Gladrow DA. 2007. The effect of iron availability on the regulation of inorganic carbon acquisition in the coccolithophore *Emiliania huxleyi* and the significance of cellular compartmentation for stable carbon isotope fractionation. *Geochimica et Cosmochimica Acta* **71**: 5301–5312.

Sekino K, Shiraiwa Y. 1994. Accumulation and utilization of dissolved inorganic carbon by a marine unicellular coccolithophorid, *Emiliania huxleyi*. *Plant and Cell Physiology* **35**: 353–361.

Sikes CS, Roer RD, Wilbur KM. 1980. Photosynthesis and coccolith formation – inorganic carbon-sources and net inorganic reaction of deposition. *Limnology and Oceanography* **25**: 248–261.

Soto AR, Zheng H, Shoemaker D, Rodriguez J, Read BA, Wahlund TM. 2006. Identification and preliminary characterization of two cDNAs encoding unique carbonic anhydrases from the marine alga *Emiliania huxleyi*. *Applied and Environmental Microbiology* **72**: 5500–5511.

Spalding MH. 2008. Microalgal carbon-dioxide-concentrating mechanisms: chlamydomonas inorganic carbon transporters. *Journal of Experimental Botany* **59**: 1463–1473.

Stoll MHC, Bakker K, Nobbe GH, Haese RR. 2001. Continuous-flow analysis of dissolved inorganic carbon content in seawater. *Analytical Chemistry* **73**: 4111–4116.

Suffrian K, Schulz KG, Gutowska MA, Riebesell U, Bleich M. 2011. Cellular pH measurements in *Emiliania huxleyi* reveal pronounced membrane proton permeability. *New Phytologist* **190**: 595–608.

Tachibana M, Allen A, Kikutani S, Endo Y, Bowler C, Matsuda Y. 2011. Localization of putative carbonic anhydrases in two marine diatoms, *Phaeodactylum tricornutum* and *Thalassiosira pseudonana*. *Photosynthesis Research* **109**: 205–221.

Taylor AR, Chrachri A, Wheeler G, Goddard H, Brownlee C. 2011. A voltage-gated H^+ channel underlying pH homeostasis in calcifying coccolithophores. *Plos Biology* **9**: e1001085.

Thierstein HR, Geitzenauer KR, Molfino B, Shackleton NJ. 1977. Global synchroneity of late Quaternary coccolith datum levels validation by oxygen isotopes. *Geology* **5**: 400–404.

Trimborn S, Langer G, Rost B. 2007. Effect of varying calcium concentrations and light intensities on calcification and photosynthesis in *Emiliania huxleyi*. *Limnology and Oceanography* **52**: 2285–2293.

Trimborn S, Wolf-Gladrow D, Richter K-U, Rost B. 2009. The effect of pCO_2 on carbon acquisition and intracellular assimilation in four marine diatoms. *Journal of Experimental Marine Biology and Ecology* **376**: 26–36.

Vandesompele J, De Preter K, Pattyn F, Poppe B, Van Roy N, De Paepe A, Speleman F. 2002. Accurate normalization of real-time quantitative RT-PCR

data by geometric averaging of multiple internal control genes. *Genome Biology* **3**: research0034.0031–research0034.0011

Wang Y, Spalding MH. 2006. An inorganic carbon transport system responsible for acclimation specific to air levels of CO_2 in *Chlamydomonas reinhardtii*. *Proceedings of the National Academy of Sciences, USA* **103**: 10110–10115.

Wolf-Gladrow DA, Riebesell U, Burkhardt S, Bijma J. 1999. Direct effects of CO_2 concentration on growth and isotopic composition of marine plankton. *Tellus Series B Chemical and Physical Meterology* **51**: 461–476.

Zeebe RE, Wolf-Gladrow D. 2001. *CO_2 in seawater: equilibrium, kinetics, isotopes*. Amsterdam, the Netherlands: Elsevier.

Supporting Information

Additional supporting information may be found in the online version of this article.

Fig. S1 Physiological response parameters for *Emiliania huxleyi* in relation to pH_f and CO_3^{2-}.

Fig. S2 *Emiliania huxleyi* PIC production, POC production and growth rates plotted against DIC.

Table S1 Target and endogenous reference gene information

Table S2 Applied statistics to physiological and gene expression data

Table S3 Tabulated values for the carbonate system, physiological response and gene expression from all experiments

Please note: Wiley-Blackwell are not responsible for the content or functionality of any supporting information supplied by the authors. Any queries (other than missing material) should be directed to the *New Phytologist* Central Office.